Applied Physics Letters

Observing non-equilibrium state of transport through graphene channel at the nano-second time-scale

Cite as: Appl. Phys. Lett. **111**, 263101 (2017); https://doi.org/10.1063/1.5006258
Submitted: 23 September 2017 • Accepted: 01 December 2017 • Published Online: 26 December 2017

Abhishek Mishra, Adil Meersha, Srinivasan Raghavan, et al.

AIP Publishing

Observing non-equilibrium state of transport through graphene channel at the nano-second time-scale

Abhishek Mishra,[1,2,a)] Adil Meersha,[1] Srinivasan Raghavan,[2] and Mayank Shrivastava[1,b)]
[1]*Department of Electronic Systems Engineering, Indian Institute of Science, Bangalore 560012, India*
[2]*Centre for Nano Science and Engineering, Indian Institute of Science, Bangalore 560012, India*

(Received 23 September 2017; accepted 1 December 2017; published online 26 December 2017)

Electrical performance of a graphene FET is drastically affected by electron-phonon inelastic scattering. At high electric fields, the out-of-equilibrium population of optical phonons equilibrates by emitting acoustic phonons, which dissipate the energy to heat sinks. The equilibration time of the process is governed by thermal diffusion time, which is few nano-seconds for a typical graphene FET. The nano-second time-scale of the process keeps it elusive to conventional steady-state or DC measurement systems. Here, we employ a time-domain reflectometry-based technique to electrically probe the device for few nano-seconds and investigate the non-equilibrium state. For the first time, the transient nature of electrical transport through graphene FET is revealed. A maximum change of 35% in current and 50% in contact resistance is recorded over a time span of 8 ns, while operating graphene FET at a current density of 1 mA/μm. The study highlights the role of intrinsic heating (scattering) in deciding metal-graphene contact resistance and transport through the graphene channel. *Published by AIP Publishing*. https://doi.org/10.1063/1.5006258

Extraordinary electrical properties of graphene have opened up new avenues in electrical[1–3] and quantum systems.[4–6] In a FET architecture, these properties are adversely affected by electric fields and interface (metal-graphene and substrate-graphene). The high electric field in the channel increases the population of optical phonons, which in turn cause excessive self-heating[7] and early velocity saturation, overall making the transport more diffusive. The intricate metal-graphene interface has been widely studied and found to be a major performance-killer.[8] This interface also shows a strong dependence on temperature.[9] The substrate-graphene interface plays a vital role in deciding thermal transport through graphene and the substrate.[10] Note that the field-dependent phonon population and metal/substrate graphene interface show dependence on temperature; therefore, a coupling among them and a transient state of electro-thermal non-equilibrium are expected at elevated temperatures, which generally occurs during high field electron transport. Since transport of heat plays a dominant role in the transient non-equilibrium state, only the investigations resolved at the time-scale comparable to phonon or heat transport along the channel can give details hidden in the transient state. Such an investigation is of vital importance in applications where switching or signal propagation happens at a very small time-scale. Few such applications include graphene nano-ribbon-based interconnects[11] and graphene-based RF transistors.[12] In this contribution, we explore the electro-thermal non-equilibrium state of graphene FET (GFET) by electrically probing the device at very small time-scales. In order to ascertain the temporal limits of the transfer of heat, we invoke the thermal network of GFET, as shown by lumped models of thermal resistance (R) and capacitance (C) in Fig. 1(d). In each branch of the network, a transient state of thermal non-equilibrium exists from $t = 0^+$ to $t = RC$ ($=l^2/\alpha$, where l is the length along which the transfer of heat happens and α is the thermal diffusivity of the material) and the branch with maximum RC defines the temporal resolution of the thermal network. For a micron-long graphene sheet ($\alpha \sim 10^{-4}$ $m^2\ s^{-1}$)[13] resting on 285 nm thick SiO_2 ($\alpha \sim 10^{-7}$ $m^2\ s^{-1}$), the calculation of the RC product reveals a thermal diffusion time of $\sim$10 ns across SiO_2[14] and $\sim$200 ps across the graphene channel.[15] Therefore, the temporal resolution of the GFET is around 10 ns. Motivated by this time-scale, we electrically probe the device for few nano-seconds.

Electrical measurements on GFETs at a smaller time-scale were earlier reported as a technique to investigate the effect of charge-trapping on saturation characteristics of the transistor.[16–18] Time-resolution of those measurements was

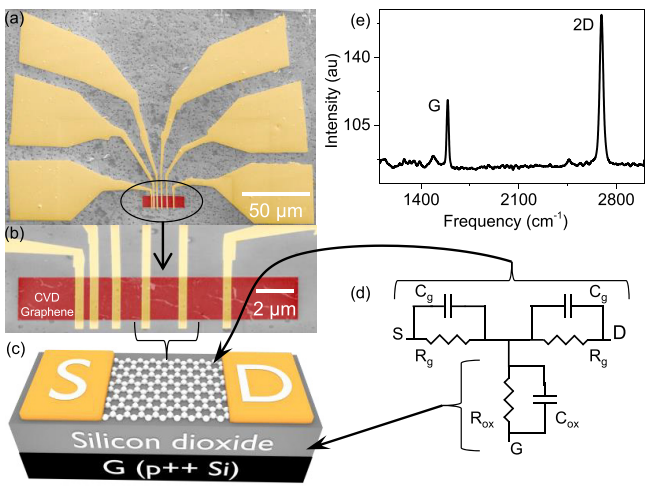

FIG. 1. (a) and (b) False color SEM image of TLM-based GFETs used in this work. (c) Schematic of the GFET and corresponding thermal network in (d). R_g and C_g represent the lumped thermal resistance and capacitance, respectively, for lateral conduction of heat through graphene, while R_{ox} and C_{ox} represent the same parameters for vertical conduction of heat through SiO_2. 3D conduction of heat is not considered, as it plays a dominant role in GNRs only.[21] (e) 2D/G > 1 and suppressed D peak in Raman spectra highlight the monolayer coverage.

a)Electronic mail: mishra@iisc.ac.in
b)Electronic mail: mayank@iisc.ac.in. URL: http://mayank.dese.iisc.ac.in/.

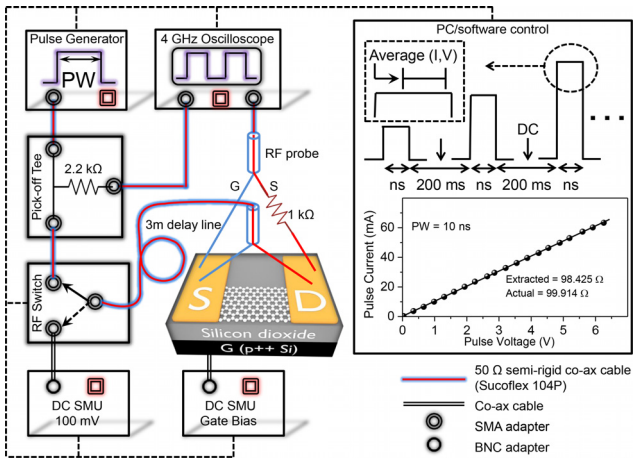

FIG. 2. TDR-based technique to perform nano-second time-scale measurements. The system is set-up in 50 Ω matched, 4 GHz environment. Termination of the transmission line at graphene FET acts as a point of reflection, due to which the device experiences a sum of incident (i) and reflected (r) waves. The 3 m long delay line inserts sufficient time-lag for the oscilloscope to capture the two waves. The total voltage (V) experienced by GFET is then given by $V_{GFET} = V_i + V_r$; while current (I) is given by $I_{GFET} = I_i - I_r = V_i/50 - V_r/50$, where the negative sign is used to account for the change in the direction of the current and 50 corresponds to input impedance of the oscilloscope. The current-voltage plot corresponding to a particular measurement set is extracted by averaging the respective transient responses from 70% to 90% of the pulse width and henceforth referred to as pulse current and pulse voltage, respectively. The pulse-to-pulse delay was fixed to 200 ms, during which the device was left to cool-down to ambient temperature. Before performing measurements on GFETs, the system was calibrated against standard passive devices. In all measurements, rise time was fixed to 600 ps, while the fall time of 1–2 ns was used.

limited to hundreds of nano-seconds, which in turn made the measurements insensitive to the electro-thermal non-equilibrium state of the GFET. Ramamoorthy *et al*. had employed a rapid pulsing system to achieve drift velocities in the range of 10^8 cm/s.[19] Although the reported system was able to apply electric fields for sub-10 ns duration to accelerate carriers to high velocities, the transient response of electro-thermal transport was not adequately captured due to limitations of the set-up, which involved repetitive sampling of a large number of transient waveforms. Measurements performed in a repetitive manner put a blanket on any transient behavior, while stressing the device multiple times with the same electric field. Investigation of the transient behavior requires stressing through a single pulse, where a pulse corresponding to a particular voltage is applied only once, and the transient data corresponding to voltage and current are precisely captured. In this work, we circumvent the limitations of measurement systems reported so far, including DC and pulse, and investigate nano-second time-resolved transport through GFET, while injecting and analyzing "single" transient waveform corresponding to a particular current-voltage value. Note that conventional steady-state or DC measurement systems require few milli-seconds to acquire a current-voltage data point and hence cannot be used to capture events happening at the nano-second time-scale. Here, we deploy an ultra-fast transient technique known as time-domain reflectometry (TDR)[20] to perform nano-second time-scale electrical measurements on GFETs (Fig. 2). Measurements were performed by injecting a set of discrete electrical pulses through GFET by RF probes. The voltage pulses were injected using a 50 Ω RF probe, while the corresponding response was sensed by a 1 kΩ RF probe. Note that instead of using wire-bonds, the devices are directly probed through RF probes, which negates the effect of parasitic inductance from wire-bonds. Moreover, 50 Ω matching across the system, semi-rigid SMA with uniform silver-plated copper wire (Sucoflex 104P), and precise calibration suppress the effect of parasitic elements. In every set, the pulse-width and gate-voltage were kept fixed, while the drain-source voltage was monotonically increased. GFETs were electrically probed through multiple measurement sets, each with different pulse-widths and gate voltages. Low-bias (100 mV) device resistance was extracted during the inter-pulse delay period, variation in which was used as an indication of high-field induced degradation. Devices showing change in the low-bias resistance were not used for the analysis. The measurement system set-up in this fashion enables precise capture of both voltage and current transients during high-field transport at the time-scale of sub-10 ns. The sequence of process steps followed for fabricating the devices used in this work is as follows: (1) transfer of graphene to the target substrate, (2) e-beam and O_2 plasma-assisted patterning of the channel, (3) e-beam patterning of contacts, and (4) metal deposition and lift-off. A total of ten devices with different values of thermal conductance were fabricated by changing the oxide thickness, channel length and width. Values of these parameters are mentioned in the succeeding discussion. Note that the measurements reported in this work were performed in a four-probe fashion, at room temperature in the ambient atmosphere.

Figure 3(a) shows the electrical response of a GFET in sub-10 ns duration. The pulse current shows a reduction with the increase in pulse time [Fig. 3(c)]. Such a dependence of current on time indicates the presence of coupling between the electron transport and non-equilibrium phenomenon. Possible reasons behind the time-dependent reduction in current are (1) trapping/de-trapping of charge carriers in the dielectric, (2) gradual degradation of the GFET, and (3) propagation of scattering-induced heat across the device. Charge trapping/de-trapping in the dielectric happens at the time-scale of micro-seconds to milli-seconds,[16] which is beyond the excitation/capture window of our measurements, and hence, their role can be safely neglected. At high electric fields, the scattering-induced rise in temperature along with atmospheric oxygen can cause gradual oxidation of graphene. In order to determine any high-field induced oxidation of the lattice, low-bias device resistance is extracted after every pulse, as depicted in Fig. 3(b). The extracted resistance does not show any change due to the application of the high electric field across the channel, which negates any occurrence of gradual degradation of GFET. The possible role of propagation of scattering-induced heat across the device in causing time-dependent change in current is investigated by analyzing the dependence of transient reduction on thermal resistance of the substrate and graphene sheet. Polar dielectrics, underlying silicon dioxide in the present case, are known to cool down the graphene sheet via high-energy phonon relaxation through surface phonon modes.[10] The efficient cooling mechanism can transfer as high as 77% of heat from graphene to SiO_2, and remaining heat is transported to metal contacts.[22] The transfer of heat to SiO_2 also depends on thermal conductance of the substrate.[23,24] Figure 4(a) shows that transient reduction in current increases with the increase in

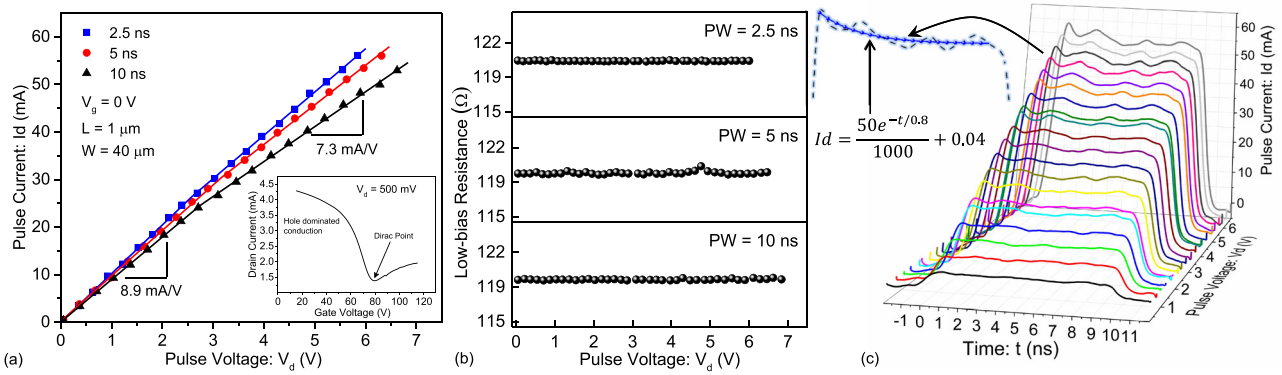

FIG. 3. (a) Pulse I-V of a GFET extracted by stressing the device by pulses of three different pulse-widths. Input characteristic shown in the inset indicates the Dirac point at ∼80 V. The characteristics fit nicely into two linear regions and henceforth referred to as high-field (HF) and low-field (LF) regions. (b) Low-bias (100 mV) DC resistance extracted after each pulse remains constant throughout the measurement cycle, which precludes the occurrence of any high-bias induced degradation. (c) Transient waveforms show exponential reduction in current at higher pulse voltages. The exponential decay dies-out in few nano-seconds. Note that the figures correspond to the same device and the same measurement cycle. Various device and electrical parameters are mentioned in (a).

thermal resistance of SiO_2. This indicates that at a given applied field, heat-flow to the substrate scales with thermal conductance of the underlying dielectric. Consequently, higher reduction in current is observed in the case of graphene resting on the dielectric with higher thermal resistance. Interestingly, the transient reduction in current decreases with the increase in thermal resistance of the graphene channel [Fig. 4(b)]. This anomalous behavior can be attributed to reduction in population of optical phonons with the decrease in the electric field across the channel. The dependence of transient reduction on thermal conductance corroborates the role of coupling between electrical and thermal transport in deciding the transient reduction in current during the non-equilibrium state.

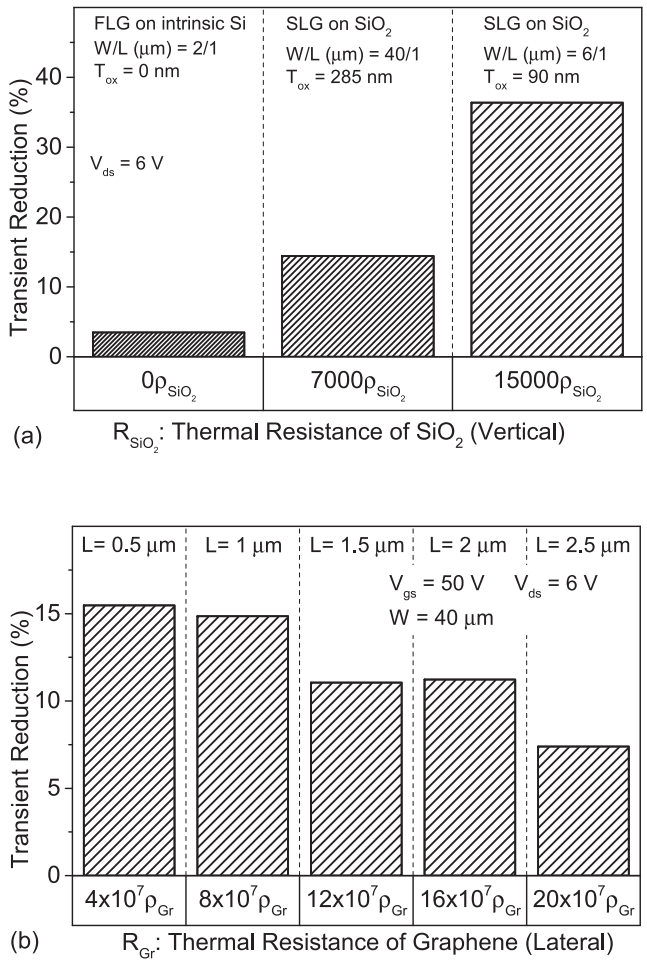

FIG. 4. Variation in transient reduction in current $\left(\frac{I_{2.5ns}-I_{10ns}}{I_{2.5ns}} \times 100\right)$ with thermal resistance of SiO_2 (a) and thermal resistance of graphene (b). Here, $R_{SiO_2} = \frac{\rho_{SiO_2} T_{ox}}{W \times L}$ and $R_{Gr} = \frac{\rho_{Gr} L}{W \times t}$, where ρ_{SiO_2} and ρ_{Gr} denote the thermal resistivity of silicon dioxide and graphene, respectively, $t = 0.3$ nm is the thickness of monolayer graphene, while W and L are the channel width and channel length, respectively.

As discussed earlier, thermal diffusion time across SiO_2 is of the order of nano-seconds, while the same across graphene is of the order of pico-seconds. The investigation of transient reduction in current in Fig. 3(c) indicates a decay time of few nano-seconds, which reveals the dominant role of thermal resistance of the substrate over that of graphene in governing the transient behavior of transport. From the preceding discussion, it is clear that thermal diffusion time of the underlying substrate plays a key role in deciding transport through GFET. However, it is still not clear why coupling between electrical and thermal transport during the non-equilibrium state results in transient reduction in current. In order to elucidate the reason behind transient reduction, we investigate the transient change in electrical parameters by extracting the channel and contact resistance at different time instants. TLM-based extraction shows the change in the channel and contact resistance with time (Fig. 5), across different gate voltages (Fig. 6). This observation indicates that heat generated in the channel interacts with the metal-graphene interface. Scattering due to high electric fields creates a near-adiabatic state, during which thermal energy remains localized at the scattering site and does not interact with the system. Thereafter, the device makes a transition from the near-adiabatic state to the electro-thermal non-equilibrium state, during which the scattering-induced thermal energy propagates to regions with a lower population of energetic phonons. The ensuing transfer of thermal energy equilibrates the system and the device strives to achieve a state of electro-thermal equilibrium. In the entire process, the device makes a transition from near-adiabatic to a state of electro-thermal equilibrium [Fig. 5(c)], and the dynamic change in population of phonons results in a transient change in electro-thermal transport. The change is captured through time-variation in current, while its origin is investigated through the corresponding change in channel resistance and contact resistance.

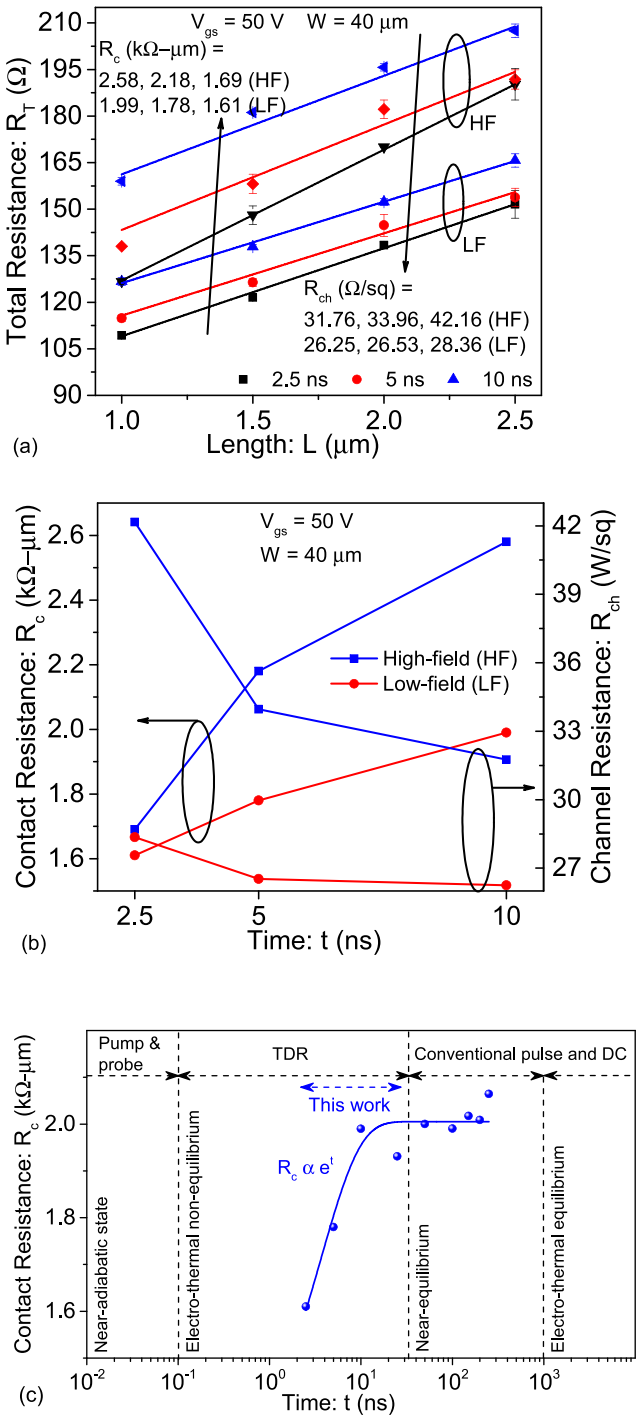

FIG. 5. (a) TLM extraction of contact and channel resistance of GFET operating in low-field and high-field regions. Contact (R_c) and channel (R_{ch}) resistances are extracted through linear fit of total resistance to $R_T = \frac{R_{ch}L}{W} + 2R_c$. (b) Both R_c and R_{ch} show dependence on time and tend to saturation with the increase in time. (c) Transient variation of average R_c shown with different electro-thermal states (and their respective measurement techniques) of a GFET.

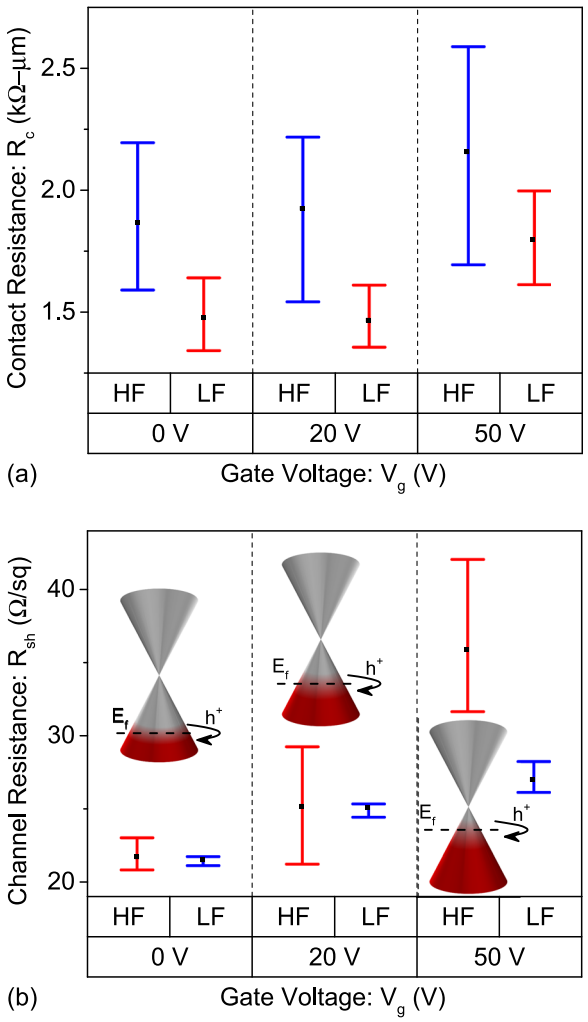

FIG. 6. Time-variation (shown by bars) and gate voltage dependence of contact (a) and channel resistance (b) of GFETs, extracted through the transfer length method and recorded from 2 ns to 10 ns. The time-variation increases as the gate voltage approaches the Dirac point. (b) Also shows a change in the hole concentration near the Fermi level, which is attributed to the scattering-assisted change in temperature.

In order to further substantiate the observed change in contact and channel resistance, we give a phenomenological description of electro-thermal transport. The high field transport through CVD-graphene is predominantly diffusive. Transfer efficiency across the metal-graphene interface is given by $\sqrt{\lambda/\lambda_m}$, where λ is the mean free path for the diffusive transport through the graphene sheet and λ_m is the coupling length along which the charge transfer happens across the interface.[9] A fraction of optical phonons relax into acoustic phonons, which in turn propagate to contacts and increase the anharmonicity of the lattice. The consequent increase in anharmonicity of the lattice decreases the interaction between p-orbitals of graphene and d-orbitals of the metal,[25,26] which eventually increases the coupling length (λ_m). In the high-field region, the mean free path is fixed by optical phonons and hence λ can be assumed to have a weak dependence on temperature. Overall, the increase in λ_m and constant mean free path (λ) results in a reduction in transfer efficiency and an increase in contact resistance. A similar temperature-dependence of the metal-graphene interface was earlier reported as a consequence of extrinsic heating.[9] Here, we observe that intrinsic heating, caused by scattering-induced generation of phonons, can also modify the metal-graphene interface. Apart from contact resistance, the channel resistance also shows a reduction with time. The reduction, albeit meager, highlights the role of temperature in changing transport through the channel. The slight reduction in channel resistance can be attributed to the increase in the intrinsic carrier concentration with temperature,[27] which in turn increases with time. The intrinsic carrier concentration is given by $n_i = \left(\frac{E_f}{\hbar v_F}\right)^2/\pi$, where v_F is the

Fermi velocity and the Fermi level E_f can be approximated as $\alpha T(V_{sd})$.[28] The n_i varies as a square of Fermi level and attains minimum at the Dirac point. Ideally, conductivity at the Dirac point should be zero but impurities and temperature result in non-zero conductivity at the Dirac point.[29] Therefore, the maximum variation in channel resistance is expected near the Dirac point. A similar behavior is shown in Fig. 6(b), where time-variation in channel resistance is shown for different gate voltages, with the maximum variation recorded near the Dirac point. Note that the observed reduction in channel resistance due to the temperature assisted increase in the carrier concentration is limited by scattering induced degradation in mobility.[30] Therefore, the channel resistance does not show a strong dependence on scattering-induced rise in temperature.

The above observation of contact heating should be contrasted with the dynamics of hot-spot equilibration reported earlier. Lateral spread of hot-spot in a GFET is decided by thermal healing length, which in turn is quantified as $L_H = \sqrt{\kappa W h/g}$, where κ is the thermal conductivity, W is the width of the device, h is the thickness of the graphene sheet (=3.35 Å), and g is the thermal conductance of the substrate per unit length.[21,31] The expression suggests that the lateral spread of heat is restricted to 300 nm only. The channel lengths discussed here are more than 1 μm; consequently, the contacts should never heat-up. Contrary to this, the extracted values of contact resistance show dependence on temperature. In order to understand the possible reason behind the contact heating, in spite of having channel lengths much larger than thermal healing lengths, we re-visit the source of heat generation in a GFET. As discussed earlier, lattice heating is initiated by emission of optical phonons by energetic electrons. The dominant phonon modes in the device are 180 meV (graphene optical phonons)[31] and 60 meV (SiO_2 surface polar phonons),[32] which indicates that optical phonons will be emitted at every 40 nm and 12 nm of length (assuming 5 V across 1 μm channel).[33] Consequently, the entire channel will be uniformly heated. The temperature profile for such a uniform heating was earlier captured through IR imaging.[34] Emission of these phonons in the vicinity of contacts eventually results in heating of the metal-graphene interface. Moreover, the concept of thermal healing should be valid for a localized hot-spot only, where only phonons of a local region are out-of-equilibrium, which equilibrate with rest of the lattice and substrate, over a length decided by thermal healing length. In the present case, a major fraction of phonons throughout the lattice are out-of-equilibrium, which in turn equilibrate through metal contacts and underlying substrate over a time period given by RC of the SiO_2 substrate.

In summary, we have investigated electro-thermal transport during the non-equilibrium state of graphene FET. The non-equilibrium state features scattering-induced rise in temperature, which in turn increases metal-graphene contact resistance and enhances electron conduction near the Dirac point. The transient change was found to be a strong function of thermal conductance of the polar dielectric supporting the graphene channel. The results reveal the time-dependent conduction across the metal-graphene interface and near Dirac-point, both of which were earlier regarded as time-independent or static processes. The observation of transient nature of conduction at the nano-second time-scale highlights the importance of investigating transport during the electro-thermal non-equilibrium state of 2D materials, wherein dimensional constraints can cause strong coupling between electrical and thermal transport.

This work was financially supported by the Department of Science and Technology, Government of India (Project Grant No. SB/S3/EECE/063/2014).

[1]X. Du, I. Skachko, A. Barker, and E. Y. Andrei, Nat. Nanotechnol. **3**, 491 (2008).
[2]J. H. Seol, I. Jo, A. L. Moore, L. Lindsay, Z. H. Aitken, M. T. Pettes, X. Li, Z. Yao, R. Huang, D. Broido, N. Mingo, R. S. Ruoff, and L. Shi, Science **328**, 213 (2010).
[3]S. Ichinokura, K. Sugawara, A. Takayama, T. Takahashi, and S. Hasegawa, ACS Nano **10**, 2761 (2016).
[4]K. S. Novoselov, Z. Jiang, Y. Zhang, S. V. Morozov, H. L. Stormer, U. Zeitler, J. C. Maan, G. S. Boebinger, P. Kim, and A. K. Geim, Science **315**, 1379 (2007).
[5]Y. Zhang, Y.-W. Tan, H. L. Stormer, and P. Kim, Nature **438**, 201 (2005).
[6]L. A. Ponomarenko, F. Schedin, M. I. Katsnelson, R. Yang, E. W. Hill, K. S. Novoselov, and A. K. Geim, Science **320**, 356 (2008).
[7]E. Pop, S. Sinha, and K. E. Goodson, Proc. IEEE **94**, 1587 (2006).
[8]K. Nagashio, T. Nishimura, K. Kita, and A. Toriumi, in *2009 IEEE International Electron Devices Meeting (IEDM)* (2009), pp. 1–4.
[9]F. Xia, V. Perebeinos, Y.-M. Lin, Y. Wu, and P. Avouris, Nat. Nanotechnol. **6**, 179 (2011).
[10]Z.-Y. Ong and E. Pop, Phys. Rev. B **84**, 075471 (2011).
[11]J. Jiang, J. Kang, W. Cao, X. Xie, H. Zhang, J. H. Chu, W. Liu, and K. Banerjee, Nano Lett. **17**, 1482–1488 (2017).
[12]J. Zheng, L. Wang, R. Quhe, Q. Liu, H. Li, D. Yu, W.-N. Mei, J. Shi, Z. Gao, and J. Lu, Sci. Rep. **3**, 1314 (2013).
[13]H. Cabrera, D. Mendoza, J. Benítez, C. B. Flores, S. Alvarado, and E. Marín, J. Phys. D: Appl. Phys. **48**, 465501 (2015).
[14]M. Berger and G. Burbach, in *1991 IEEE International SOI Conference Proceedings* (1991), pp. 24–25.
[15]Z. Xu and M. J. Buehler, J. Phys.: Condens. Matter **24**, 475305 (2012).
[16]Y. G. Lee, C. G. Kang, U. J. Jung, J. J. Kim, H. J. Hwang, H.-J. Chung, S. Seo, R. Choi, and B. H. Lee, Appl. Phys. Lett. **98**, 183508 (2011).
[17]K. Majumdar, S. Kallatt, and N. Bhat, Appl. Phys. Lett. **101**, 123505 (2012).
[18]I. Meric, C. R. Dean, A. F. Young, N. Baklitskaya, N. J. Tremblay, C. Nuckolls, P. Kim, and K. L. Shepard, Nano Lett. **11**, 1093 (2011).
[19]H. Ramamoorthy, R. Somphonsane, J. Radice, G. He, C.-P. Kwan, and J. P. Bird, Nano Lett. **16**, 399 (2016).
[20]Y. Wang, K. P. Cheung, R. Choi, G. A. Brown, and B. H. Lee, IEEE Electron Device Lett. **28**, 279 (2007).
[21]A. D. Liao, J. Z. Wu, X. Wang, K. Tahy, D. Jena, H. Dai, and E. Pop, Phys. Rev. Lett. **106**, 256801 (2011).
[22]M. Freitag, M. Steiner, Y. Martin, V. Perebeinos, Z. Chen, J. C. Tsang, and P. Avouris, Nano Lett. **9**, 1883 (2009).
[23]M.-H. Bae, S. Islam, V. E. Dorgan, and E. Pop, ACS Nano **5**, 7936 (2011).
[24]S. Islam, Z. Li, V. E. Dorgan, M. H. Bae, and E. Pop, IEEE Electron Device Lett. **34**, 166 (2013).
[25]A. Meersha, H. B. Variar, K. Bhardwaj, A. Mishra, S. Raghavan, N. Bhat, and M. Shrivastava, in *2016 IEEE International Electron Devices Meeting (IEDM)* (2016), pp. 5.3.1–5.3.4.
[26]M. Ghatge and M. Shrivastava, IEEE Trans. Electron Devices **62**, 4139 (2015).
[27]Q. Shao, G. Liu, D. Teweldebrhan, and A. A. Balandin, Appl. Phys. Lett. **92**, 202108 (2008).
[28]Y. Yin, Z. Cheng, L. Wang, K. Jin, and W. Wang, Sci. Rep. **4**, 5758 (2014).
[29]J. Martin, N. Akerman, G. Ulbricht, T. Lohmann, J. H. Smet, K. von Klitzing, and A. Yacoby, Nat. Phys. **4**, 144 (2008).
[30]S. Sarkar, K. R. Amin, R. Modak, A. Singh, S. Mukerjee, and A. Bid, Sci. Rep. **5**, 16772 (2015).
[31]E. Pop, V. Varshney, and A. K. Roy, MRS Bull. **37**, 1273 (2012).
[32]X. Li, E. A. Barry, J. M. Zavada, M. B. Nardelli, and K. W. Kim, Appl. Phys. Lett. **97**, 232105 (2010).
[33]Z. Yao, C. L. Kane, and C. Dekker, Phys. Rev. Lett. **84**, 2941 (2000).
[34]T. E. Beechem, R. A. Shaffer, J. Nogan, T. Ohta, A. B. Hamilton, A. E. McDonald, and S. W. Howell, Sci. Rep. **6**, 26457 (2016).